Ultracold three-body collisions near narrow Feshbach resonances

Yujun Wang, J. P. D'Incao, and B. D. Esry

Phys. Rev. A **83**, 042710 — Published 25 April 2011

DOI: 10.1103/PhysRevA.83.042710

Ultracold three-body collisions near narrow Feshbach resonances

Yujun Wang,[1,*] J. P. D'Incao,[2] and B.D. Esry[1]

[1]*Department of Physics, Kansas State University, Manhattan, Kansas, 66506, USA*
[2]*JILA, University of Colorado and NIST, Boulder, Colorado, 80309-0440, USA*

We study ultracold three-body collisions of bosons and fermions when the interatomic interaction is tuned near a narrow Feshbach resonance. We show that the width of the resonance has a substantial impact on the collisional properties of ultracold gases in the strongly interacting regime. From our numerical and analytical analyses, we identify universal features dependent on the resonance width. Remarkably, we find that all inelastic processes near narrow resonances leading to deeply bound states in bosonic systems are suppressed while those for fermionic systems are enhanced. As a result, narrow resonances present a scenario the reverse of that found for broad resonances, opening up the possibility of creating stable samples of ultracold bosonic gases with large scattering lengths.

PACS numbers:

I. INTRODUCTION

Strongly interacting three-body systems play an important role in many areas of physics, extending over condensed matter, atomic, molecular, and nuclear physics [1, 2]. Advances in the control of interatomic interactions have made ultracold atomic gases a preferred test bed for many interesting physical phenomena. One of the most important tools for this control is the magnetic- or optical-Feshbach resonance [3, 4]. Applying an external field, the s-wave scattering length a between two atoms can be tuned from $-\infty$ to $+\infty$. Although the tunability of the interatomic interaction greatly expands the range of experimentally accessible phenomena, a major difficulty encountered in the strongly interacting limit, $|a| \gg r_0$ where r_0 is the characteristic range of the interatomic interactions, is that the system can become unstable due to three-body collisional losses of atoms and molecules. An exception to that rule is a two-component Fermi gas, which shows extraordinary stability against few-body losses near a Feshbach resonance [5–9], allowing the experimental realization of a broad range of novel physical phenomena [10].

The fundamental few-body physics behind the theoretical understanding of the stability of bosonic and fermionic gases is related to Efimov physics [11, 12]. In fact, in the past few years, few-body physics has received a great deal of attention due to the experimental verification of several key features of Efimov physics [13–22], confirming our understanding of this intriguing universal phenomena. Nevertheless, most of the universal phenomena explored so far, except the ones in Ref. [23–30], relies on the assumption that ultracold scattering properties depend only on a, which is expected to be a good one for broad Feshbach resonances. That can be easily understood given the low-energy expansion of the two-body s-wave scattering phase shift δ,

$$k_2 \cot\delta = -\frac{1}{a} + \frac{1}{2} r_{\rm eff} k_2^2 + \ldots, \tag{1}$$

where k_2 is the two-body wavenumber and $r_{\rm eff}$ is the effective range. When $k_2 \ll \sqrt{2/|a r_{\rm eff}|}$, the scattering length a is the only quantity needed to characterize the two-body scattering properties. In this paper, however, we focus on narrow resonances where this condition does not apply. For the magnetic Feshbach resonances used in ultracold experiments, $r_{\rm eff}$ can be estimated from the resonance parameters by [23, 31]

$$r_{\rm eff} = -\frac{1}{|\mu_2 a_{\rm bg} \Delta\mu \Delta B|}, \tag{2}$$

where μ_2 is the two-body reduced mass, $a_{\rm bg}$ is the background scattering length, $\Delta\mu$ is the difference of the magnetic moment between the two channels involved in the resonance, and ΔB is the resonance width in the magnetic field. The effective ranges for some selected Feshbach resonances [4] are listed in Table I in App. B. Since $|r_{\rm eff}|$ is inversely proportional to the resonance width [23], the second term in Eq. (1) is negligible at low collisional energies for broad resonances. Near a narrow resonance, however, $|r_{\rm eff}| \gg r_0$ and the second term in Eq. (1) is no longer negligible for three-body collisions even at ultracold collision energies. This implies that $r_{\rm eff}$ should be incorporated in the three-body universal theory for the narrow resonances.

Although some authors regard three-body "universality" as the determination of three-body properties by the scattering length alone, universality can be more broadly defined to include the dependence of three-body properties on a few parameters that encapsulate the details of the short-range interactions. As we will show here, the role of a large effective range is similar to that of the scattering length in the sense that it *universally* affects the behavior of a three-body system.

Narrow resonances are expected not only to affect the underlying Efimov physics [23, 24] but also have consequences for the BEC-BCS crossover picture for fermionic

*Present address: JILA, University of Colorado, 440 UCB, Boulder, Colorado, 80309, USA

systems [32]. In fact, the possibility of new many-body physics near narrow Feshbach resonances has been proposed theoretically in Refs. [33, 34]. Furthermore, the closed-channel-dominant nature of a narrow Feshbach resonances may give novel few-body physics, since the two-body wavefunction always carry strong bound state characteristics even if they do not form a bound state. Therefore, understanding the role of the effective range is crucial. While specific systems have been modeled near a resonance [26, 27, 35, 36], no simple analytical expressions for scattering observables near narrow resonances, like those for broad resonances [2, 37, 38], have yet been obtained.

We believe that a better understanding of the physics near narrow resonances becomes increasingly important since narrow Feshbach resonances are frequently encountered in gases with mixed atomic species in many recent experiments [39–42]. Since the scattering lengths and effective ranges in a heteronuclear system can take quite different values for distinct pairs by tuning through overlapping resonances [43], a rich variety of three-body physics is expected to arise in such systems. Moreover, the development of optical Feshbach resonances techniques [44–46] promises greater experimental control over the width of the resonance. It is thus important to develop the universal theory for the three-body physics near narrow resonances.

Our goal with this paper is to provide the general framework for such a theory and derive explicit formulas for the scattering observables that properly incorporate the dependence on $r_{\rm eff}$. In particular, we study the dependence of ultracold three-body collision rates on $r_{\rm eff}$, obtaining analytic expressions for K_3 and $V_{\rm rel}$ similar to those already obtained for broad resonances [see Eqs. (13) and (14)]. Moreover, we verify these expressions with numerical solutions. Surprisingly, we find that *all* inelastic processes leading to deeply-bound two-boson states are suppressed as $|r_{\rm eff}|^{-1}$, indicating that bosonic gases can be more stable near narrow resonances. In contrast, we find that fermionic gases should be less stable due to enhanced losses for large $|r_{\rm eff}|$.

We use atomic units throughout this paper unless otherwise stated.

II. THEORY

A. Background

Most of the current understanding of three-body physics near narrow Feshbach resonances has been based on the zero-range potential model (ZRP) [47] which, despite imposing many convenient simplifications, makes it difficult to evaluate the importance of the short-range physics. The two main implementations of ZRP to study three-body physics are by Petrov [23] and Gogolin *et. al* [24]. In particular, Petrov calculated the recombination rate for identical bosons near a narrow Feshbach resonance with $a>0$ using a modified ZRP to include $r_{\rm eff}$ [23]. By solving his model numerically, he found that the minima described by Eq. (12) still appear for $a \gg |r_{\rm eff}|$ but occur at fixed values of $|r_{\rm eff}|/a$ without any reference to the three-body parameter Φ, indicating that the three-body physics is solely determined by a and $r_{\rm eff}$. Gogolin *et al.* [24] reproduced these results with a very different method but effectively the same physical model. Other theoretical efforts seek to address the modification of Efimov physics by the effective range [28–30] but are restricted to $|r_{\rm eff}| \approx r_0$ such that their perturbative treatment remains adequate. Their results, therefore, cannot be applied to narrow Feshbach resonances.

More fundamentally, and in contrast to [23] and [24], we show that the short-range three-body physics is in fact important near a narrow resonance for identical bosons — even in the limit $r_0 \to 0$. Petrov and Gogolin *et al.* took advantage of the fact that the inclusion of $r_{\rm eff}$ in the ZRP model regularizes the three-body dynamics, eliminating the mathematical need for a three-body short-range parameter. This regularization had been investigated earlier in Ref. [48] and was recently revisited in [49]. While the Thomas collapse [50] is avoided by including $r_{\rm eff}$ in the ZRP model, we will show both numerically and analytically that a three-body parameter is still needed to represent the short-range three-body physics and that, consequently, a and $r_{\rm eff}$ alone are insufficient to describe ultracold three-body observables. Below, we will describe our model used to implement variations of $r_{\rm eff}$ in our numerical calculations.

B. Modeling Feshbach resonances

Feshbach resonances [4] are a multi-channel phenomenon. In general, a two-channel model is sufficient to reproduce the main resonant structure contained in the real problem. Roughly speaking, a Feshbach resonance occurs when a state of the closed (upper) channel becomes degenerate with the collision energy of two free atoms in the open (lower) channel, as illustrated in Fig. 1(a). In ultracold gases, the tunability afforded by a magnetic Feshbach resonance of interactions is achieved by tuning the separation of the asymptotic thresholds of the two channels such that the scattering length in the lower channel goes through a pole when the closed channel state moves across the threshold of the open channel. The width of the resonance, and therefore the effective range [see Eq. (2)], are mainly controlled by the strength of the coupling between the open and closed channels. Generally, strong coupling produces broad Feshbach resonances (small $|r_{\rm eff}|$); and weak coupling, narrow resonances (large $|r_{\rm eff}|$).

If there is only one open channel, one can design a single channel model that has the same asymptotic scattering wavefunction as the multi-channel wavefunction at ultracold collision energies. Such a model is possible since the asymptotic wavefunction does not depend on

the short-range two-body physics that generates the resonance [23, 51]. We thus model the Feshbach resonance with a single-channel potential that supports a shape resonance as shown in Fig. 1(b). Specifically, we use

$$V_{\rm sech}(r) = -D{\rm sech}^2(3r/r_0) + Be^{-2(3r/r_0-2)^2}, \quad (3)$$

where r is the distance between the two atoms. The potential depth D primarily controls a, and the barrier height B is adjusted to produce the desired $r_{\rm eff}$. Instead of coupling two different channels as in the Feshbach resonance case, our model couples the scattering region ($r > r_0$) with the short-range region ($r < r_0$). We use $r_0 \approx 50$ a.u. in all of our numerical calculations.

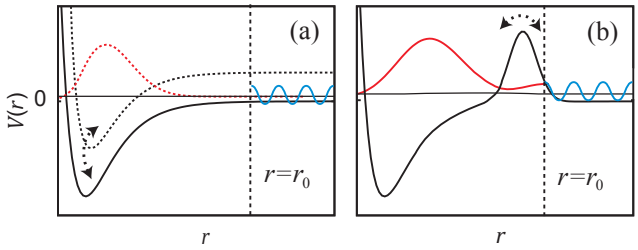

FIG. 1: Schematic comparison of a Feshbach resonance (a) and a shape resonance (b). On resonance, the short-range ($r < r_0$), bound component is similar in both cases and the long-range ($r > r_0$) wavefunction is the same. The double-headed arrows indicate the coupling.

In order to investigate the three-body universality, i.e., universal properties that do not depend on a particular choice of model interaction, we have also used a two-body potential consisting of the sum of a Morse potential and a Gaussian barrier, given by

$$V_{\rm Morse}(r) = D[(1-e^{-(3r/r_0-1)})^2-1] + Be^{-2(3r/r_0-2)^2}. \quad (4)$$

C. Adiabatic hyperspherical representation

We solve the three-body Schrödinger equation using the adiabatic hyperspherical representation [52]. In this representation, the overall size of the three-body system is characterized by the hyperradius R, and the three-body configuration is represented by a set of hyperangles Ω.

After scaling the three-body wavefunction Ψ by $\psi = R^{5/2}\Psi$, the Schrödinger equation can be written as

$$\left[-\frac{1}{2\mu}\frac{\partial^2}{\partial R^2} + H_{\rm ad}(R;\Omega)\right]\psi = E\psi, \quad (5)$$

where E is the total energy, $\mu = m/\sqrt{3}$ is the three-body reduced mass. We solve Eq. (5) by first expanding the three-body wavefunction as

$$\psi = \sum_{\nu=0}^{\infty} F_{\nu E}(R)\Phi_\nu(R;\Omega), \quad (6)$$

where the adiabatic channel functions $\Phi_\nu(R;\Omega)$ are solutions of the adiabatic equation

$$H_{\rm ad}\Phi_\nu = U_\nu(R)\Phi_\nu, \quad (7)$$

solved for fixed values of R. Here $U_\nu(R)$ is the adiabatic hyperspherical potential. Upon substitution of ψ, Eq. (5) reduces to a set of coupled one-dimensional equations:

$$\left[-\frac{1}{2\mu}\frac{d^2}{dR^2} + U_\nu\right]F_{\nu E} - \frac{1}{2\mu}\sum_{\nu'}\left[2P_{\nu\nu'}\frac{d}{dR} + Q_{\nu\nu'}\right]F_{\nu' E} = EF_{\nu E}, \quad (8)$$

with non-adiabatic couplings $P_{\nu\nu'}$ and $Q_{\nu\nu'}$ defined by

$$P_{\nu\nu'}(R) = \left\langle\!\!\left\langle \Phi_\nu \left| \frac{d}{dR} \right| \Phi_{\nu'} \right\rangle\!\!\right\rangle, \quad (9)$$

$$Q_{\nu\nu'}(R) = \left\langle\!\!\left\langle \Phi_\nu \left| \frac{d^2}{dR^2} \right| \Phi_{\nu'} \right\rangle\!\!\right\rangle. \quad (10)$$

Here, the double brackets denote integration over only the hyperangular degrees of freedom. The hyperspherical adiabatic representation, therefore, offers a simple and conceptually clear description of three-body scattering processes. The non-adiabatic couplings drive the inelastic collisions between channels characterized by the effective potentials

$$W_{\nu\nu}(R) = U_\nu(R) - \frac{1}{2\mu}Q_{\nu\nu}(R), \quad (11)$$

which in turn support all bound states and resonances of the system and dictate many of the scattering properties of the system. Here, we obtain the scattering observables by solving Eq. (8) using the R-matrix method [53], while the analytical properties are derived primarily based on the properties of the effective potentials.

III. THREE-BODY INELASTIC PROCESSES FOR IDENTICAL BOSONS

For an atomic sample with spin-stretched bosons B in their lowest hyperfine state, it is well known that the atomic losses are dominated by three-body recombination, $B+B+B \to B_2+B$, releasing enough kinetic energy for collision products to escape from the trap. For $|a| \gg r_0$ near a broad Feshbach resonance, the three-body recombination rates K_3 have the following universal expressions [2, 37, 38]:

$$K_3^{(a>0)} = 67.1e^{-2\eta}\left(\sin^2[s_0\ln\frac{a}{r_0}+\Phi]+\sinh^2\eta\right)\frac{a^4}{m}, \quad (12)$$

$$K_3^{(a<0)} = \frac{4590\sinh 2\eta}{\sin^2[s_0\ln(|a|/r_0)+\Phi+1.53]+\sinh^2\eta}\frac{a^4}{m}, \quad (13)$$

where $s_0 \approx 1.00624$, Φ is a short-range three-body phase, and η is a parameter that represents the probability of

inelastic transitions to deeply bound dimers at short distances. While the overall behavior of K_3 is determined by a, any comparison with experimental data requires the short-range three-body parameters Φ and η to be properly determined. In general, these three-body parameters can not be predicted from two-body physics alone [54], and must be determined by fitting some three-body observable.

If weakly-bound molecules B_2^* are present, their lifetime is determined by atom-dimer relaxation processes, $B_2^*+B\rightarrow B_2+B$ [2]. The vibrational relaxation rate $V_{\rm rel}$ also has a universal form when $a>0$ and $a\gg r_0$:

$$V_{\rm rel}=\frac{20.3\sinh 2\eta}{\sin^2[s_0\ln(a/r_0)+\Phi+1.47]+\sinh^2\eta}\frac{a}{m}. \qquad (14)$$

When $a<0$, $V_{\rm rel}$ is independent of a.

A. Numerical inelastic rates

One implicit, reasonable, assumption behind the universal expressions Eqs. (12) and (13) is that the three-body potentials and couplings at short distances ($R\lesssim r_0$) remain practically unchanged when the scattering length is tuned through a pole. Similarly, to extract the universal behavior of a three-body system with large effective range, we also want to have negligible changes in the short-range physics when the effective range is tuned. Otherwise, the universal scaling behavior will be unphysically entangled with the non-universal changes of the short-range physics. With $V_{\rm sech}$ and $V_{\rm Morse}$, however, a non-negligible change in the barrier height is required to make a large when $r_{\rm eff}$ is changed through a large range. This leads to non-negligible changes for the short-range physics. To solve this problem, we introduced a hard wall in $W_{\nu\nu}(R)$ at R=r_0 to cut-off the non-universal short-range behavior. The behavior of the potentials $W_{\nu\nu}(R)$ beyond R=r_0 are universal, allowing us to extract the universal properties of the scattering observables. To confirm that the insertion of the hard wall at $R=r_0$ does not lead to undesired effects, we have verified that our numerical results are not sensitive to the precise location of this hard wall.

1. *Three-body recombination for $a>0$*

Figure 2 shows our numerical calculations of K_3 when $a>0$. We generated each curve by varying a at fixed $|r_{\rm eff}|$, mimicking the tuning of magnetic field across a Feshbach resonance for the cases where $|r_{\rm eff}|$ does not change significantly across the resonance. For $a\gg|r_{\rm eff}|$, the rates retain the features predicted in Eq. (12), due to the fact that the scaling behavior of the inelastic rates should still be determined by Efimov physics when a is the largest length scale in the system. For $a\lesssim|r_{\rm eff}|$, however, K_3 deviates from this formula and approaches the $(a^7|r_{\rm eff}|)^{1/2}$

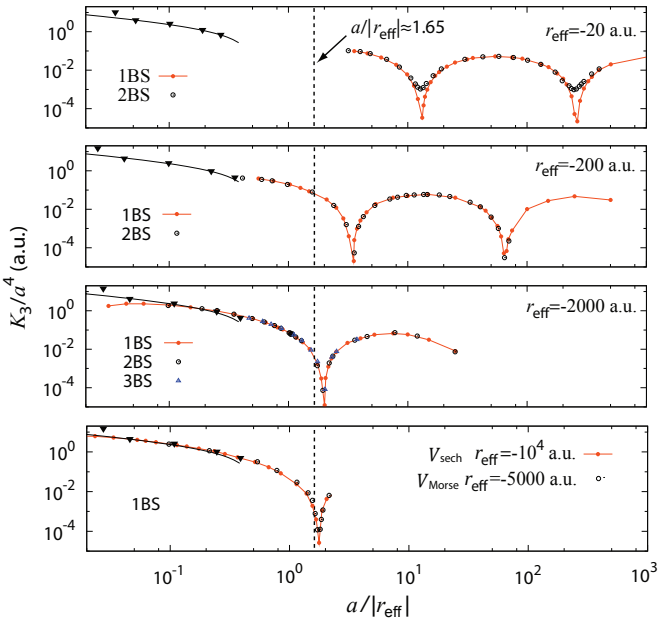

FIG. 2: Ultracold three-body recombination rates for identical bosons ($a>0$). The vertical dashed lines indicate the position of the first Efimov feature predicted in Refs. [23, 24]. The solid triangles are experimental data for the 907G Feshbach resonance in a Na BEC [55]. Here we show K_3 with one or more two-body s-wave bound states (BS), including the analytical result from [23] scaled to match our data (thick solid line). In the lowest panel we show the recombination rates calculated by using two different two-body potentials: the potential defined in Eq. (3) and (4). Here r_0=50 a.u..

behavior predicted in [23] [see black solid line in Fig. 2]. The figure also shows that the rates seem to converge to a universal curve as $|r_{\rm eff}|$ increases. Moreover, as the limit $r_0/|r_{\rm eff}|\rightarrow 0$ is approached, the position of the first Efimov minimum as a function of $|a|/|r_{\rm eff}|$ agrees reasonably well with the ZRP predictions from Refs. [23] and [24]. However, as will be discussed later, this agreement should not be generally expected. In any case, Table I shows that $r_{\rm eff}$ is typically below 10^3 a.u. for those resonances with a few gauss of width. Therefore typical experiments will actually fall far from range of validity of the ZRP results since $r_0\sim 100$ a.u.. Thus, for the moderate values of $|r_{\rm eff}|$ in typical experiments, Fig. 2 shows that the positions of the minima in $a/|r_{\rm eff}|$ deviate dramatically from the ZRP prediction. It followed that any experimental attempt to reduce atomic losses by tuning the ratio $a/|r_{\rm eff}|$ close to a minimum in K_3 will require knowledge of the short-range three-body physics just as for broad resonances.

One interesting observation in Fig. 2 is that the minima in K_3 for more than one two-body bound state become more pronounced, i.e., the value of K_3 at a minimum decreases as $|r_{\rm eff}|$ increases. If there were a single weakly bound two-body state, K_3 would vanish at the minimum. When deeply bound states are available to

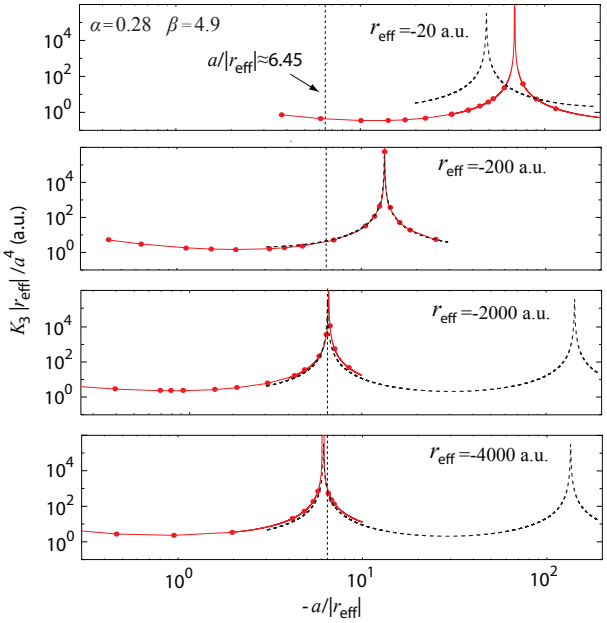

FIG. 3: Ultracold three-body recombination rates ($a < 0$) for identical bosons. The solid lines through the numerical data points are to guide the eye, while the dashed lines are the analytical results from Eq. (21), using the α and β indicated from a fit in the limit $|r_{\rm eff}|\to\infty$. Here r_0=50 a.u..

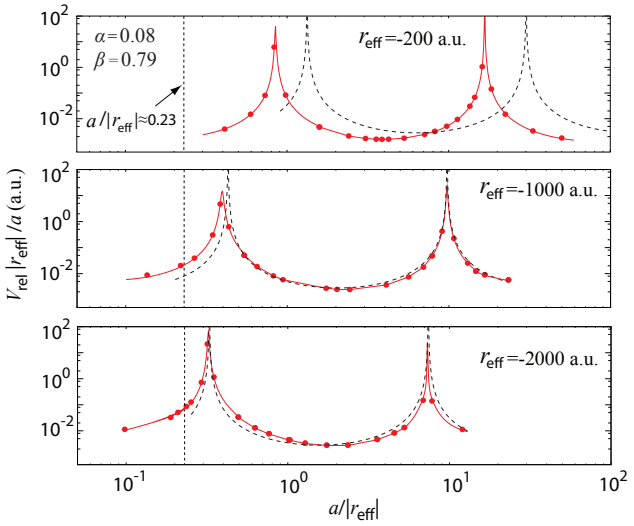

FIG. 4: Ultracold three-body relaxation rates ($a > 0$) for identical bosons. The solid lines through the numerical data points are to guide the eye, while the dashed lines are the analytical results from Eqs. (16), respectively, using the α and β indicated from a fit in the limit $|r_{\rm eff}|\to\infty$. Here r_0=50 a.u..

recombine into, however, K_3 no longer vanishes at the minima. This situation can be clearly seen in Fig. 2 when $|r_{\rm eff}| \approx r_0$. The deeper minima for larger $|r_{\rm eff}|$, therefore, indicate the suppression of recombination into deeply-bound states. As will be discussed later, this suppression is the consequence of a new scaling behavior with large $|r_{\rm eff}|$.

2. *Three-body recombination for $a < 0$*

In Fig. 3, we show K_3 for $a < 0$. The rates are scaled as $K_3|r_{\rm eff}|/a^4$ to show the overall scaling with $|r_{\rm eff}|$. Similar to K_3 for $a > 0$, the numerical rates are calculated by changing a with a fixed $r_{\rm eff}$. When $|r_{\rm eff}|$ increases, the curves converge to a limiting case, and we compare the positions for the first peak in K_3 with its ZRP prediction. In particular, the K_3 prediction is based on the scattering length when the first Efimov state becomes bound [24]. It can be seen that this prediction is close to our limiting position, but is not in exact agreement.

3. *Three-body relaxation for $a > 0$*

In Fig. 4, we show the scaled numerical relaxation rate $V_{\rm rel}|r_{\rm eff}|/a$ for $a > 0$, calculated by changing a with a fixed $r_{\rm eff}$. The curves again show convergent behavior to a limiting case, and the prediction on the position for the first peak is based on the position of the first pole in the atom-dimer scattering length in [23]. The position in our numerical calculation is seemingly approaching the prediction, but the agreement is not clear. One important feature in Figs. 3 and 4 is that the rates for each inelastic process have similar magnitude when multiplied by $|r_{\rm eff}|$, which indicates a $1/|r_{\rm eff}|$ suppression in both of the inelastic processes.

B. Adiabatic potentials and analytical results

A common property of there-body recombination ($a < 0$) and relaxation ($a > 0$) is that the couplings between the initial and final channels are significant only at short range. Inelastic transitions for these processes thus predominantly occur when $R \lesssim r_0$. To understand the $1/|r_{\rm eff}|$ scaling behavior, we study the properties of the corresponding adiabatic hyperspherical potentials. This approach has proven successful for processes near broad resonances since the adiabatic potentials and their couplings have proven to be universal [56]. In App. A, we discuss the scaling behavior of the adiabatic potentials in ZRP model, and show the inadequacy of this model in deriving the adiabatic potentials for narrow resonances. In this section, we will discuss scaling behavior of the potentials based on our numerical calculations.

In the following we study the universal scaling of the adiabatic potentials and their couplings for $|a| \gg |r_{\rm eff}|$. The scalings for $|a| \ll |r_{\rm eff}|$ is more involved and will not be discussed in this paper. Figure 5 shows the idealized $W_{\nu\nu}(R)$ for three identical bosons with $r_0 \ll |r_{\rm eff}| \ll |a|$ [57]. The potentials are exactly the same as for a

broad resonance except in the range $r_0 \ll R \ll |r_{\rm eff}|$. In this range, $W_{\nu\nu}(R)$ for the weakly-bound atom-dimer channel takes the Coulomb-like form [23, 58]:

$$W_{\nu\nu} = \frac{c_0}{2\mu_3 |r_{\rm eff}| R} \tag{15}$$

instead of the usual attractive $1/R^2$ Efimov potential. The Coulomb-like behavior is what remains after a cancellation of the $1/R^2$ leading order terms in the potential $U_\nu(R)$ by the diagonal correction $-Q_{\nu\nu}/2\mu$ in Eq. (11). For broad Feshbach resonances, the diagonal correction $Q_{\nu\nu}/2\mu$ is proportional to $1/R^3$ in the region $r_0 \ll R \ll |a|$ [56] and as a result it does not cancel the attractive $1/R^2$ coming from $U_\nu(R)$. For narrow resonances, although the adiabatic potentials $U_\nu(R)$ still have the Efimov behavior when $r_0 \ll R \ll |a|$, $Q_{\nu\nu}/2\mu$ is instead proportional to $1/R^2$ in the region $r_0 \ll R \ll |r_{\rm eff}|$ and surprisingly washes away the Efimov behavior in the potential in this region. Studies [49] have shown that this new behavior in $Q_{\nu\nu}/2\mu$ comes from a non-universal short-range component of the two-body wavefunction in the regions where two atoms are close to each other, which is absent in the ZRP treatments. Indeed, our numerical analysis indicates that the coefficient c_0 in Eq. (15) is not universal. As shown in Fig. 6, c_0 can change from positive to negative values depending on the number of deeply bound states. This indicates that the potentials in the region $R \ll |a|$ are not universal.

When $R \gg |r_{\rm eff}|$ the potentials recover the universal Efimov behavior. This non-universality of the three-body effective potentials makes it surprising that the inelastic rates in Figs. 2–4, calculated with different model potentials and different number of two-body bound states, are universal.

To better understand the origin of this universal behavior, we use our idealized potentials $W_{\nu\nu}(R)$ shown in Fig. 5 to derive analytic expressions for the collision rates. Based on our experience on analyzing broad resonances, the inelastic rates from full numerical calculations are expected to agree with the analytical expressions when the prerequisites of the universal scaling hold: $r_0 \ll |r_{\rm eff}| \ll |a|$. Empirically, the relation "$\ll$" here typically means more than one order of magnitude, which is similar to the prerequisite $r_0 \ll |a|$ for broad Feshbach resonances [56]. For the purpose of deriving simple analytic expressions, we use $\alpha|r_{\rm eff}|$ and $\beta|a|$ [59] to quantify the boundaries of the hyperradial regions, as shown in Fig. 5. The universal parameters α and β will be determined by fitting our final expression to the numerical results. As shown in Fig. 5, the non-universal region $r_0 \ll R \ll |r_{\rm eff}|$ requires special handling. In principle, we can retain the Coulomb-like potential. But, recognizing that its effective charge $c_0/2\mu|r_{\rm eff}|$ is small and the sign/value of c_0 does not affect the numerical rates, we simply set the potential in our model to be zero in the region $r_0 \ll R \ll |r_{\rm eff}|$. Therefore, the only effect of the existence of the Coulomb-like region is to physically separate the short-range region and the Efimov region.

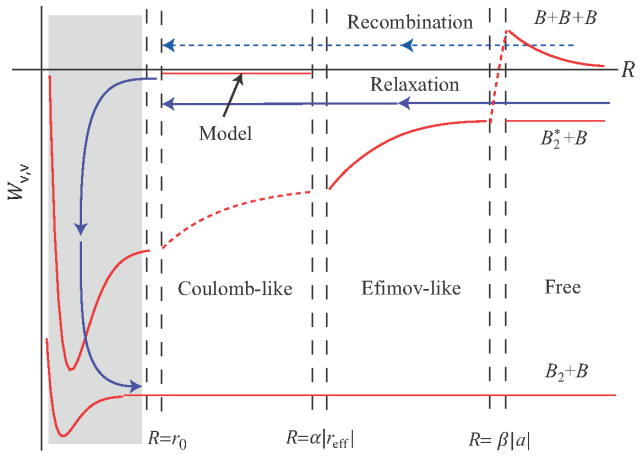

FIG. 5: Schematic $W_{\nu\nu}(R)$ used to derive Eq. (16) and (21) with $r_0 \ll |r_{\rm eff}| \ll |a|$. The difference in the potentials between the recombination ($a < 0$) and relaxation ($a > 0$) is only in the asymptotic region. In the "Coulomb-like" region, the potential shown in dashed line is attractive only when there is one or two two-body bound states in the system. The short-range region is shadowed to indicate strong coupling between the initial and final channels, where inelastic transition occur dominantly.

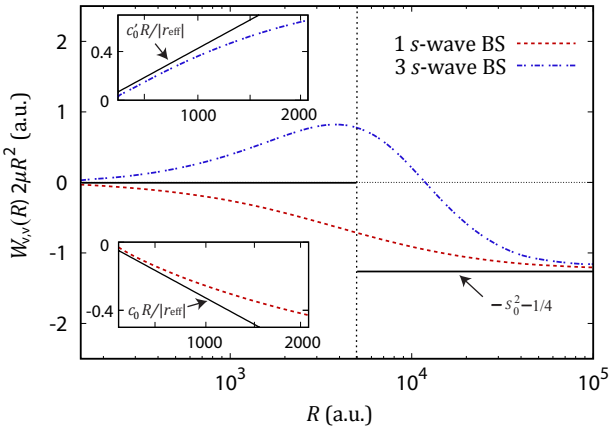

FIG. 6: Adiabatic hyperspherical potentials near a narrow Feshbach resonance. Numerical $W_{\nu\nu}(R)$ multiplied by $2\mu R^2$ with $r_{\rm eff}$=–5000 a.u. and $|a|=\infty$. The lower curve is from the calculations with a single $2+1$ s-wave bound channel and the upper one is from the calculations with three $2+1$ s-wave bound channels.

As with any analytic treatment of universal three-body processes, the short-range three-body physics must be parametrized. For instance, in Eqs. (12)–(14) for broad resonances, the three-body physics for $R \lesssim r_0$ is parametrized by Φ and η. For the narrow resonance considered here, we will instead use a complex three-body short-range scattering length A, where the real part ReA characterizes the low-energy elastic scattering and the imaginary part ImA accounts for the short-range inelas-

tic transitions to deeply-bound two-body states. This choice permits us to write the final expressions in a form that most closely resembles Eqs. (13)–(14). We calculate $V_{\rm rel}$ by considering incidence in the weakly-bound atom-dimer channel with the transition to the deeper two-body channels driven by the non-adiabatic coupling localized in the region $R \lesssim r_0$. The derivation of the analytic rates is detailed in App. C. Briefly, the hyperradial wavefunction is written down in each region, then matched at the boundaries. The relaxation rate for identical bosons is then obtained from $V_{\rm rel}^{(B)}=\pi(1-\mathcal{R})/\mu k$ where $\mathcal{R}$ is the elastic scattering probability, yielding

$$V_{\rm rel}^{(B)} = \frac{2\sqrt{3}\pi\beta \sin 2\varphi_0 \sinh 2\eta}{\sin^2[s_0 \ln(|a/r_{\rm eff}|) + \Phi + \varphi] + \sinh^2 \eta} \frac{a}{m} \quad (16)$$

where

$$\tan\Phi = 2s_0 \frac{\alpha - {\rm Re}A/|r_{\rm eff}|}{\alpha + {\rm Re}A/|r_{\rm eff}|}, \quad (17)$$

$$\sinh\eta = \left|\frac{{\rm Im}A}{\alpha r_{\rm eff}}\right| \csc(2\varphi_0)\sin^2(\Phi+\varphi_0), \quad (18)$$

and

$$\varphi = s_0 \ln(\beta/\alpha) + \varphi_0, \quad (19)$$

$$\tan\varphi_0 = \frac{s_0}{l+1/2}. \quad (20)$$

The effective angular momentum [60] refers to the initial channel, and is $l=0$ for relaxation.

With a virtually identical analysis, $K_3^{(a<0)}$ for $r_0 \ll \alpha|r_{\rm eff}| \ll \beta|a|$ can be derived to be

$$K_3^{(a<0)} = \frac{12\sqrt{3}\pi^3\beta^4 \sin 2\varphi_0 \sinh 2\eta}{\sin^2[s_0 \ln(|a/r_{\rm eff}|) + \Phi + \varphi] + \sinh^2 \eta} \frac{a^4}{m}. \quad (21)$$

Note that since different Hamiltonian apply — one for $a<0$ and one for $a>0$ — α and β can take different values for $V_{\rm rel}^{(B)}$ and K_3. The effective angular momentum in this case is $l=3/2$ [60] for the lowest three-body continuum channel. Similar expressions can be derived for other low-energy scattering observables.

In Figs. 3 and 4, the values of α and β are fitted from the $|r_{\rm eff}|$-dependence of the peak positions in the numerical $V_{\rm rel}$ and $K_3^{(a<0)}$, in the universal limit $|r_{\rm eff}| \gg r_0$. The analytic results show converging behavior to the numerical calculations in the universal limit $|r_{\rm eff}| \gg r_0$. One interesting point is that the universal limit is approached at smaller value of $|r_{\rm eff}| \gg r_0$ for $K_3^{(a<0)}$ than for $V_{\rm rel}$. For $K_3^{(a<0)}$, the analytic results is almost on top of the numerical ones when $|r_{\rm eff}|/r_0=4$, whereas significant deviation is observed in $V_{\rm rel}$ at the same value of $|r_{\rm eff}|/r_0$.

The comparison of Eqs (16) and (21) with Eqs. (14) and (13), respectively, shows that r_0 is replaced by $\alpha|r_{\rm eff}|$, as one would expect with the introduction of a new length scale smaller than $|a|$. There are, however, additional non-trivial modifications that cannot be predicted by this simple replacement. Our expressions above explain, for instance, the scaling of the rates with $|r_{\rm eff}|$ used in Figs. 3 and 4: the factor $\sinh 2\eta$ introduces a $|r_{\rm eff}|^{-1}$ suppression. This reduction of η, which is connected to transitions to deeply-bound two-body states, is also responsible for the more pronounced minima in Fig. 2 as $|r_{\rm eff}|$ increases for those calculations with multiple two-body bound states. The observation of interference minima in K_3 is thus more favorable near a narrow Feshbach resonance, in the sense it will be more pronounced under the same experimental conditions.

Equations (16) and (21) further reveal the fundamental importance of the short-range three-body physics through their dependence on A in both η and Φ. This physics is absent from the zero-range treatments [23, 24], so the agreement in Figs. 3 and 4 between our numerical results and the ZRP predictions for the position of the first Efimov feature is rather fortuitous. We see from the arguments of $\sin^2$ in Eqs. (16) and (21) that A-independent Efimov feature positions — as predicted in [23, 24] — are found only in the limits $|{\rm Re}A/r_{\rm eff}|\to 0$ and $|{\rm Re}A/r_{\rm eff}|\to\infty$. Since A represents short-range three-body physics, it should remain approximately constant near a Feshbach resonance but can vary from system to system. For all of the numerical examples shown above ${\rm Re}A \sim r_0$ due to the presence of the hard wall added at $R\sim r_0$. Consequently, the limit $r_0/r_{\rm eff}\to 0$ yields universal Efimov feature positions. Also, since ${\rm Re}A$ remains constant for each value of $r_{\rm eff}$ in Fig. 2, Φ from Eq. (18) is independent of the number of two-body bound states, placing the Efimov features in the same positions. This need not be true in general, however. In particular, if there is a short-range three-body resonance near the break-up threshold, the value of ${\rm Re}A$ can, in principle, take any value from $-\infty$ to $+\infty$.

For a broad resonance, the short-range phase Φ in Eqs. (12)–(14) corresponds to the phase in the hyperradial wavefunction $F_{\nu E}(R)$ at $R=r_0$ if one assumes that $F_{\nu E}(R)$ takes the following form near $R=r_0$:

$$F_{\nu E}(R) \propto \sqrt{R}\sin[s_0 \ln(R/r_0) + \Phi + i\eta]. \quad (22)$$

For a narrow resonance, the phase Φ in Eqs. (16) and (21) instead gives the phase of $F_{\nu E}(R)$ at $R=\alpha|r_{\rm eff}|$, with $F_{\nu E}(R)$ taking the same form as Eq. (22) near $R=\alpha|r_{\rm eff}|$. The parameter η for a narrow resonance gives an "effective" loss parameter for all losses at $R \le \alpha|r_{\rm eff}|$ with essentially the same physical interpretation as the η parameter for a broad resonance. In the limit $\alpha|r_{\rm eff}|\to r_0$, both Φ and η for a narrow resonance reduce to those for a broad resonance, under the assumption that $\eta \ll 1$. In this limit, we can determine the value of β for a broad resonance, by comparing the phases in Eqs. (16) and (21) to those in Eqs. (14) and (13). This gives β=1.4 for relaxation and β=2.9 for recombination.

IV. VIBRATIONAL RELAXATION FOR FERMIONIC SYSTEM

To show that the present analysis of narrow resonances is more general than the identical boson system discussed so far, we will consider a two-component Fermi system with a narrow interspecies Feshbach resonance. If the components correspond to the same atomic isotope in different hyperfine states, say F and F', three-body processes are in general suppressed near an interspecies Feshbach resonance. For recombination, this suppression is a consequence of the Pauli exclusion principle applied to the FFF' system. In particular, K_3 for $F+F+F' \to (FF')^*+F$ is proportional to k^2 near zero energy, where $k=\sqrt{2\mu E}$ is the incident wavenumber and E is the collision energy [60]. Therefore, in the ultracold regime, three-body recombination vanishes for FFF' systems, and we restrict our study to vibrational relaxation since its rate is constant as $k \to 0$. Nevertheless, in this case, the rate for atom-dimer relaxation, $(FF')^*+F \to FF'+F$, is suppressed as $1/a^{3.33}$ [9, 12], an important property since it stabilizes atom-molecule fermionic mixtures.

To get a sense of the effect of large $|r_{\rm eff}|$ on fermionic collisions, we have studied the atom-dimer relaxation processes near narrow resonances. For broad resonances, i.e., $|r_{\rm eff}| \simeq r_0$, the usual $a^{-3.33}$ suppression on $V_{\rm rel}^{(F)}$ [9] originates from a repulsive barrier in the incident adiabatic hyperspherical potential

$$W_{\nu\nu}(R) \simeq \frac{p_0^2-1/4}{2\mu R^2} \tag{23}$$

in the range $r_0 \ll R \ll a$ [12]. The universal constant $p_0 \approx 2.166$ is determined by a transcendental equation from the ZRP model [61, 62].

When $|r_{\rm eff}| \gg r_0$, however, $W_{\nu\nu}(R)$ is modified in the range $r_0 \ll R \ll |r_{\rm eff}|$ by the emergence of a Coulomb-like potential, similar to what was found for bosons. However, the coefficient for the Coulomb-like potential for fermions $c_0 \approx 0.3$ and does not change when the number of s-wave bound states between F and F' is increased. Nevertheless, compared with the potential in Eq. (23), the modified repulsive barrier is weakened due to the smallness of the effective charge in the Coulomb-like potential, leading to an *enhancement* of vibrational relaxation. Moreover, when $a \ll |r_{\rm eff}|$, the dependence of the rate on a is altered, much like for bosons with $a \ll |r_{\rm eff}|$ in Fig. 2. All of these effects can be seen in our numerical calculations shown in Fig. 7. For $a<|r_{\rm eff}|$, the numerical result shows that relaxation scales as $(a/|r_{\rm eff}|)^{-1}$, a much weaker suppression than for broad resonances.

For $a>|r_{\rm eff}|$, we can apply the same kind of analysis as for bosons, using the fact that the idealized potential behaves as in Eq. (23) for $|r_{\rm eff}| \ll R \ll a$ and assuming the potential is zero for $r_0 \ll R \ll |r_{\rm eff}|$. We obtain for this case

$$V_{\rm rel}^{(F)} = \frac{256\pi\sqrt{3}p_0^2\,|{\rm Im}A|/m}{[(1-4p_0^2)({\rm Re}A/|\alpha r_{\rm eff}|)^2+(2p_0+1)^2]^2}\left[\frac{\beta a}{|\alpha r_{\rm eff}|}\right]^{1-2p_0}. \tag{24}$$

We recover the broad resonance scaling with a, $V_{\rm rel}^{(F)} \propto (a/|r_{\rm eff}|)^{-3.33}$ when $r_{\rm eff}<0$, but with a much larger overall magnitude due to the dependence on $r_{\rm eff}$.

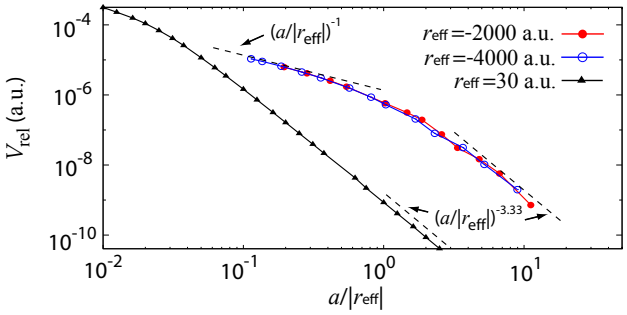

FIG. 7: Relaxation rates for mixed-spin fermions with $a>0$ and large $|r_{\rm eff}|$. The relaxation rate for small $|r_{\rm eff}|$ is also plotted, showing the same scaling with a but not with $|r_{\rm eff}|$ since it is not in the universal limit.

V. SUMMARY

We have studied ultracold collisions of three identical bosons and of mixed-spin fermions near a narrow Feshbach resonance using the connection between $r_{\rm eff}$ for the two-body interaction and the width of the resonance. We were able to identify the key modifications to the three-body adiabatic hyperspherical potentials and thus derive analytical expressions for the rate constants. From these analytical expressions, we showed that short-range three-body physics is still important, even near a narrow Feshbach resonance. This result is, perhaps, unfortunate for experimentalists since the positions of the Efimov features are, in general, still dependent on short-range physics, making it difficult to locate *a priori* a minimum of K_3 as suggested in [23]. On the other hand, our analysis has shown that bosonic recombination and relaxation to deeply-bound two-body states are suppressed near a narrow resonance which might prove beneficial experimentally. Similarly, our analysis suggests that long-lived weakly-bound FF' molecules are most easily obtained near a broad resonance.

Appendix A: Adiabatic potentials with the zero-range potential model

The effective range has been used in Ref. [48, 57] to calculate the regularized three-body adiabatic hyperspherical potentials within ZRP model. Here we aim to study

the scaling behavior of the potentials with $r_{\rm eff}$ and show the difference between the results from a ZRP treatment and those from numerical calculations near narrow Feshbach resonances.

We extend the ZRP treatment for small effective range [47] by including up to the effective-range term in the low-energy expansion of the two-body scattering phase shift to better represent the scattering properties at finite energy:

$$\frac{\partial}{\partial r_{ij}}(r_{ij}\Psi) = \left(-\frac{1}{a} + \frac{1}{2}r_{\rm eff}k_2^2\right)\Psi \quad (r_{ij}\to 0) \qquad \text{(A1)}$$

where r_{ij} is the interparticle distance. Treating k_2^2 as proportional to two-body kinetic energy operator $\nabla^2_{\boldsymbol{r}_{ij}}$, the above boundary condition leads to the transcendental equation for the three-body adiabatic equation,

$$s_0\cosh(\frac{\pi}{2}s_0) - \frac{8}{\sqrt{3}}\sinh(\frac{\pi}{6}s_0) = 12^{-\frac{1}{4}}\sinh(\frac{\pi}{2}s_0)\left(\frac{2R}{a} + \frac{r_{\rm eff}}{R}s_0^2\right), \qquad \text{(A2)}$$

where $s_0 = s_0(R)$ is related to the adiabatic hyperspherical potential by

$$U_\nu = -\frac{s_0^2(R)+\frac{1}{4}}{2\mu R^2}. \qquad \text{(A3)}$$

As mentioned earlier, in the ZRP model, the diagonal coupling $Q_{\nu\nu}/2\mu$ is of higher order than $1/R^2$ for $R \ll |a|$ and is thus negligible in this region. The lowest effective adiabatic potential $W_{00}(R)$ then behaves like

$$W_{00}(R) \simeq -\frac{c_0}{2\mu|r_{\rm eff}|R} - \frac{1/4}{2\mu R^2}, \qquad \text{(A4)}$$

in the region $r_0 \ll R \ll |r_{\rm eff}|$ with $c_0 \approx 1.68$. Due to the largeness of $|r_{\rm eff}|$, the potential in Eq. (A4) is dominated by the $1/R^2$ term. The form of the zero-range three-body potential thus disagrees with the numerical result for the Coulomb-like potential by having an additional $1/R^2$. Further, the non-universal property of the three-body potentials seen in the numerical calculations in this region is not manifested in the ZRP potential at all. The behavior of the potentials for the continuum channels in the region $r_0 \ll R \ll |r_{\rm eff}|$, however, agrees with the numerical results. They both behave like the potentials for free particles:

$$W_{\nu\nu} = \frac{\lambda(\lambda+4)+15/4}{2\mu R^2}, \qquad \text{(A5)}$$

where λ is a non-negative integer [60]. In the Efimov region $|r_{\rm eff}| \ll R \ll |a|$ and asymptotic region $R \gg |a|$, the leading behavior of the zero-range three-body potentials agrees with the numerical results, as they both reduce to the behavior for small $|r_{\rm eff}|$ case.

Appendix B: Table of effective range for selected resonances

We list the effective range and short-range radius (r_0) for some narrow Feshbach resonances in Table I. The effective ranges are calculated using the resonance parameters (resonance position, $a_{\rm bg}$, $\Delta\mu$ and ΔB) from Ref. [4]. The short-range radius r_0 is given by the van der Waals length [2]. From Fig. 2 and 4 we observe that the ZRP results for scattering observables give reasonably predict the first Efimov features only when $|r_{\rm eff}|$ is beyond a few thousand. For the resonances listed in Table I, this implies that the ZRP results may only be applied for those with width below 1 G, given Re$A \approx r_0$ and $r_0 = 50$ a.u..

Appendix C: Single-channel approach for deriving three-body inelastic rates

To derive Eqs. (16), (21) and (24), we use a variation of the optical potential approach [63]. Optical potentials, which are non-Hermitian, have long been added to otherwise Hermitian Hamiltonians to allow flux to be lost to degrees of freedom not explicitly treated. The original Feshbach projection formalism [63] dictates the rigorous way to do this, but often the optical potential is introduced phenomenologically.

Three-body recombination and vibrational relaxation necessarily involve multiple adiabatic hyperspherical potentials and can be calculated within a multichannel scattering formalism. For recombination with $a < 0$ and relaxation with $a > 0$, however, all of the universal behavior is determined by the initial channel alone since the non-adiabatic couplings — and thus the inelastic transitions — occur predominantly in the non-universal region $R \lesssim r_0$. We can thus use the optical potential approach

Atomic species	Res. position (G)	$a_{\rm bg}$ (a.u.)	$\Delta\mu$ (μ_B)	ΔB (G)	$r_{\rm eff}$ (a.u.)	r_0) (a.u.)
^{6}Li	543.25	60	2	0.1	–71300	62.5
^{23}Na	1195	62	–0.15	1.4	–17100	89.9
^{23}Na	907	63	3.8	1	–947	”
^{23}Na	853	63	3.8	0.0025	–373000	”
^{87}Rb	1007.2	100	2.79	0.21	–1010	165
^{87}Rb	911.7	100	2.71	0.0013	–168000	”
^{87}Rb	685.4	100	1.34	0.006	–73400	”
^{87}Rb	406.2	100	2.01	0.0004	–734000	”
^{87}Rb	9.13	99.8	2.00	0.015	–19700	”
^{133}Cs	47.97	926	1.21	0.12	–287	202
^{133}Cs	19.84	160	0.57	0.005	–84600	”
^{133}Cs	53.5	995	1.52	0.0025	–10200	”
^{52}Cr	589.1	105	2	1.7	–276	91.3
^{52}Cr	499.9	107	4	0.08	–2880	”
^{39}K+^{87}Rb	317.9	34	2	7.6	–185	143

TABLE I: Effective range for some selected Feshbach resonances.

to replace all of the deeper-lying final adiabatic channels in these cases by short-range phenomenological parameters. Instead of actually modifying $W_{\nu\nu}$, though, we will use the equivalent approach of imposing a complex boundary condition at $R = r_0$ [57] where the imaginary part is related to the inelastic transition probability.

We thus begin with the schematic potential described in Fig. 5:

$$W_{\nu\nu}(R) = \begin{cases} 0 & r_0 < R < \alpha|r_{\rm eff}|, \\ -\dfrac{s_0^2+1/4}{2\mu R^2} & \alpha|r_{\rm eff}| < R < \beta|a|, \\ E_\nu + \dfrac{l(l+1)}{2\mu R^2} & R > \beta|a| \end{cases}, \quad \text{(C1)}$$

where the threshold energy for the initial channel E_ν is zero for recombination and $-1/2\mu_2 a^2$ for relaxation. The asymptotic , free-particle potential is characterized by l=0 for relaxation and l=3/2 for recombination. The parameters α and β, expected to be universal and in the order of unity, represent the fact that the boundaries between regions are not so sharply defined in practice. They can be fixed by fitting the final analytic expressions to numerical rates. By neglecting the small residual non-adiabatic couplings between the initial and the final channel for $R > r_0$, the hyperradial wavefunction in the initial channel can be written down piece-wise:

$$F_{\nu E}(R) = \begin{cases} C_1 \sin[kR + \delta_s(k)] & r_0 < R < \alpha|r_{\rm eff}|, \\ C_2\sqrt{R}[J_{is_0}(kR) + \tan\delta_2 N_{is_0}(kR)] & \alpha|r_{\rm eff}| < R < \beta|a|, \\ C_3\sqrt{R}[J_{l+1/2}(kR) + \tan\delta N_{l+1/2}(kR)] & R > \beta|a|, \end{cases} \quad \text{(C2)}$$

For $k \to 0$ and $|a| \gg |r_{\rm eff}|$, the short-range phase shift δ_s is

$$\delta_s(k) = -Ak, \quad \text{(C3)}$$

where A is the short-range three-body scattering length introduced in Sec. III B. Due to the inelastic transitions at $R \le r_0$, A acquires an imaginary part which determines the strength of the transition. Matching the hyperradial wavefunction $F_0(R)$ at $\alpha|r_{\rm eff}|$ and $\beta|a|$ gives the asymptotic phase shift δ in terms of $\alpha|r_{\rm eff}|$, $\beta|a|$ and A. The probability for elastic scattering $\mathcal{R}$ is the reflection coefficient:

$$\mathcal{R} = \left|\frac{1 + i\tan\delta}{1 - i\tan\delta}\right|^2. \quad \text{(C4)}$$

The probability for an inelastic transition is then determined as

$$1-\mathcal{R}=\frac{2\pi}{\Gamma(l+\frac{3}{2})\Gamma(l+\frac{1}{2})}\left(\frac{k\beta|a|}{2}\right)^{2l+1}\frac{\sin 2\varphi_0\sinh 2\eta}{\sinh^2\eta+\sin^2[s_0\ln(|a/r_{\rm eff}|)+\Phi+\varphi]}, \tag{C5}$$

where the parameters Φ, η, φ and φ_0 are defined in Eqs. (18)–(20). The recombination rate K_3 and the relaxation rate $V_{\rm rel}$ are expressed by the inelastic transition probability through

$$K_3=\frac{192\pi^2}{\mu k^2}(1-\mathcal{R}), \tag{C6}$$

$$V_{\rm rel}=\frac{\pi}{\mu k}(1-\mathcal{R}). \tag{C7}$$

For the mixed-spin fermionic system FFF', we are interested in the three-body relaxation process $(FF')^*+F\to FF'+F$, where $(FF')^*$ is a weakly-bound molecule and FF' is a deeply-bound molecule. Since the adiabatic hyperspherical potential for this system is different from the potential for bosons only in the region $\alpha|r_{\rm eff}|<R<\beta|a|$, we can calculate FFF' relaxation with this same formalism. Thus, $W_{\nu\nu}$ in $\alpha|r_{\rm eff}|<R<\beta|a|$ must be replaced by

$$W_{\nu\nu}(R)=\frac{p_0^2-1/4}{2\mu R^2}, \tag{C8}$$

where p_0 is the universal constant given in Sec. IV.

The corresponding hyperradial wavefunction is thus changed to

$$F_{\nu E}(R)=C_2\sqrt{R}[J_{p_0}(kR)+\tan\delta_2 N_{p_0}(kR)], \tag{C9}$$

for $\alpha|r_{\rm eff}|<R<\beta|a|$. Following exactly the same analysis as for identical bosons, we get the relaxation rate for FFF' system Eq. (24).

Acknowledgments

This work was supported by the National Science Foundation. Y. W. and J.P.D. also acknowledge the support from the National Science Foundation under Grant No. PHY0970114.

[1] A. S. Jensen, K. Riisager, D. V. Fedorov, and E. Garrido, Rev. Mod. Phys. **76**, 215 (2004).
[2] E. Braaten and H. Hammer, Physics Reports **428**, 259 (2006).
[3] H. Feshbach, Annals of Physics **19**, 287 (1962), ISSN 0003-4916.
[4] C. Chin, R. Grimm, P. Julienne, and E. Tiesinga, Rev. Mod. Phys. **82**, 1225 (2010).
[5] S. Jochim, M. Bartenstein, A. Altmeyer, G. Hendl, S. Riedl, C. Chin, J. Hecker Denschlag, and R. Grimm, Science **302**, 2101 (2003).
[6] S. Jochim, M. Bartenstein, A. Altmeyer, G. Hendl, C. Chin, J. H. Denschlag, and R. Grimm, Phys. Rev. Lett. **91**, 240402 (2003).
[7] C. A. Regal, M. Greiner, and D. S. Jin, Phys. Rev. Lett. **92**, 040403 (2004).
[8] C. A. Regal, M. Greiner, and D. S. Jin, Phys. Rev. Lett. **92**, 083201 (2004).
[9] D. S. Petrov, C. Salomon, and G. V. Shlyapnikov, Phys. Rev. Lett. **93**, 090404 (2004).
[10] S. Giorgini, L. P. Pitaevskii, and S. Stringari, Rev. Mod. Phys. **80**, 1215 (2008).
[11] V. Efimov, Physics Letters B **33**, 563 (1970), ISSN 0370-2693.
[12] J. P. D'Incao and B. D. Esry, Phys. Rev. Lett. **94**, 213201 (2005).
[13] T. Kraemer, M. Mark, P. Waldburger, J. Danzl, C. Chin, B. Engeser, A. Lange, K. Pilch, A. Jaakkola, H. Nägerl, et al., Nature **440**, 315 (2006).
[14] F. Ferlaino, S. Knoop, M. Berninger, W. Harm, J. P. D'Incao, H.-C. Nägerl, and R. Grimm, Phys. Rev. Lett. **102**, 140401 (2009).
[15] S. Knoop, F. Ferlaino, M. Mark, M. Berninger, H. Schöbel, H. Nägerl, and R. Grimm, Nature Physics **5**, 227 (2009).
[16] T. B. Ottenstein, T. Lompe, M. Kohnen, A. N. Wenz, and S. Jochim, Phys. Rev. Lett. **101**, 203202 (2008).
[17] J. H. Huckans, J. R. Williams, E. L. Hazlett, R. W. Stites, and K. M. O'Hara, Phys. Rev. Lett. **102**, 165302 (2009).
[18] G. Barontini, C. Weber, F. Rabatti, J. Catani, G. Thalhammer, M. Inguscio, and F. Minardi, Phys. Rev. Lett. **103**, 043201 (2009).
[19] M. Zaccanti, B. Deissler, C. D'Errico, M. Fattori, M. Jona-Lasinio, S. Müller, G. Roati, M. Inguscio, and G. Modugno, Nature Physics **5**, 586 (2009).
[20] N. Gross, Z. Shotan, S. Kokkelmans, and L. Khaykovich, Phys. Rev. Lett. **103**, 163202 (2009).
[21] S. Pollack, D. Dries, and R. Hulet, Science **326**, 1683 (2009).
[22] J. R. Williams, E. L. Hazlett, J. H. Huckans, R. W. Stites, Y. Zhang, and K. M. O'Hara, Phys. Rev. Lett. **103**, 130404 (2009).
[23] D. S. Petrov, Phys. Rev. Lett. **93**, 143201 (2004).
[24] A. O. Gogolin, C. Mora, and R. Egger, Phys. Rev. Lett. **100**, 140404 (2008).
[25] M. D. Lee, T. Köhler, and P. S. Julienne, Phys. Rev. A

76, 012720 (2007).
[26] G. Smirne, R. M. Godun, D. Cassettari, V. Boyer, C. J. Foot, T. Volz, N. Syassen, S. Dürr, G. Rempe, M. D. Lee, et al., Phys. Rev. A **75**, 020702 (2007).
[27] P. Massignan and H. T. C. Stoof, Phys. Rev. A **78**, 030701 (2008).
[28] E. Braaten and H.-W. Hammer, Phys. Rev. A **67**, 042706 (2003).
[29] H.-W. Hammer, T. A. Lähde, and L. Platter, Phys. Rev. A **75**, 032715 (2007).
[30] L. Platter, C. Ji, and D. R. Phillips, Phys. Rev. A **79**, 022702 (2009).
[31] G. M. Bruun, A. D. Jackson, and E. E. Kolomeitsev, Phys. Rev. A **71**, 052713 (2005).
[32] S. D. Palo, M. L. Chiofalo, M. J. Holland, and S. J. J. M. F. Kokkelmans, Physics Letters A **327**, 490 (2004), ISSN 0375-9601.
[33] O. S. Sørensen, N. Nygaard, and P. B. Blakie, Phys. Rev. A **79**, 053601 (2009).
[34] O. S. Sørensen, N. Nygaard, and P. B. Blakie, Phys. Rev. A **79**, 063615 (2009).
[35] O. I. Kartavtsev and J. H. Macek, Few-Body Systems **31**, 249 (2002).
[36] N. P. Mehta, S. T. Rittenhouse, J. P. D'Incao, and C. H. Greene, Phys. Rev. A **78**, 020701 (2008).
[37] E. Nielsen and J. H. Macek, Phys. Rev. Lett. **83**, 1566 (1999).
[38] B. D. Esry, C. H. Greene, and J. P. Burke, Phys. Rev. Lett. **83**, 1751 (1999).
[39] C. A. Stan, M. W. Zwierlein, C. H. Schunck, S. M. F. Raupach, and W. Ketterle, Phys. Rev. Lett. **93**, 143001 (2004).
[40] E. Wille, F. M. Spiegelhalder, G. Kerner, D. Naik, A. Trenkwalder, G. Hendl, F. Schreck, R. Grimm, T. G. Tiecke, J. T. M. Walraven, et al., Phys. Rev. Lett. **100**, 053201 (2008).
[41] A.-C. Voigt, M. Taglieber, L. Costa, T. Aoki, W. Wieser, T. W. Hänsch, and K. Dieckmann, Phys. Rev. Lett. **102**, 020405 (2009).
[42] K. Pilch, A. D. Lange, A. Prantner, G. Kerner, F. Ferlaino, H.-C. Nägerl, and R. Grimm, Phys. Rev. A **79**, 042718 (2009).
[43] J. P. D'Incao and B. D. Esry, Phys. Rev. Lett. **103**, 083202 (2009).
[44] J. L. Bohn and P. S. Julienne, Phys. Rev. A **56**, 1486 (1997).
[45] F. K. Fatemi, K. M. Jones, and P. D. Lett, Phys. Rev. Lett. **85**, 4462 (2000).
[46] M. Theis, G. Thalhammer, K. Winkler, M. Hellwig, G. Ruff, R. Grimm, and J. H. Denschlag, Phys. Rev. Lett. **93**, 123001 (2004).
[47] Y. N. Demkov and V. N. Ostrovskii, *Zero-Range Potentials and Their Applications in Atomic Physics* (New York : Plenum Press, 1988).
[48] D. V. Fedorov and A. S. Jensen, J. Phys. A **34**, 6003 (2001).
[49] M. Thøgersen, D. V. Fedorov, A. S. Jensen, B. D. Esry, and Y. Wang, Phys. Rev. A **80**, 013608 (2009).
[50] L. H. Thomas, Phys. Rev. **47**, 903 (1935).
[51] S. Jonsell, Journal of Physics B: Atomic, Molecular and Optical Physics **37**, S245 (2004).
[52] H. Suno, B. D. Esry, and C. H. Greene, Phys. Rev. Lett. **90**, 053202 (2003).
[53] M. Aymar, C. H. Greene, and E. Luc-Koenig, Rev. Mod. Phys. **68**, 1015 (1996).
[54] J. D'Incao, C. Greene, and B. Esry, Journal of Physics B: Atomic, Molecular and Optical Physics **42**, 044016 (2009).
[55] J. Stenger, S. Inouye, M. R. Andrews, H.-J. Miesner, D. M. Stamper-Kurn, and W. Ketterle, Phys. Rev. Lett. **82**, 2422 (1999).
[56] J. P. D'Incao and B. D. Esry, Phys. Rev. A **72**, 032710 (2005).
[57] S. Jonsell, EPL (Europhysics Letters) **76**, 8 (2006).
[58] D. S. Petrov, *Three-boson problem near a narrow feshbach resonance, talk at the workshop on strongly interacting quantum gases*, Ohio State University (April, 2005), (http://octs.osu.edu/images/Gases/Talks/Petrov.pdf).
[59] N. P. Mehta, S. T. Rittenhouse, J. P. D'Incao, J. von Stecher, and C. H. Greene, Phys. Rev. Lett. **103**, 153201 (2009).
[60] B. D. Esry, C. H. Greene, and H. Suno, Phys. Rev. A **65**, 010705 (2001).
[61] V. Efimov, Sov. J. Nucl. Phys **12**, 589 (1971).
[62] V. Efimov, Nucl. Phys. A **210**, 157 (1973).
[63] H. Friedrich, *Theoretical Atomic Physics* (Springer, 3rd Ed, 2005).